Title: Cocaine causes rapid remodeling of dopaminergic axons, synapses, and mitochondria

Authors: G.A. Wildenberg[1,2*], A.M. Sorokina [1,2], J.L. Koranda[1], A. Monical[3], C. Heer[1], M.E. Sheffield[1], X. Zhuang[1], DS McGehee[3], N. Kasthuri[1,2]

Affiliations:

[1]Department of Neurobiology, University of Chicago, Chicago, IL, USA.

[2]Argonne National Laboratory, Lemont, IL, USA.

[3]Department of Anesthesia & Critical Care, University of Chicago, Chicago, IL, USA.

*Correspondence to: gwildenberg@uchicago.edu

Summary

Detailing the ways drugs of abuse physically change dopaminergic circuits would provide new mechanisms for explaining addictive behaviors, future targets for therapeutic intervention, and insights into the nature of synaptic plasticity. We combine recent advances in genetic labeling with large volume serial electron microscopy to detail how normal dopaminergic (DA) axons interact with putative targets and how those interactions change in mice briefly exposed to cocaine. We find that while most DA boutons are devoid of obvious signs of synapses (i.e. synaptic vesicles or synaptic densities) many DA boutons physically interdigitate with both dendrites and excitatory and inhibitory axons. After a brief exposure to cocaine, we find evidence of large-scale structural remodeling: extensive axonal branching and frequent occurrences of axonal blind-ended “bulbs”, filled with mitochondria, reminiscent of axonal retraction in the developing and damaged brain. The number of physical interdigitations and vesicle filled boutons between DA axons and targets scales linearly with the length of axon whether in controls or cocaine exposed animals and the size or the type of interaction (i.e. axo-axonic or axo-dendritic) does not change. Finally, we find significant cell-type and sub-cellular specific increases in mitochondrial length in response to cocaine. Specifically, mitochondria in dopamine axons and local Nucleus Accumbens (NAc) dendrites are ~3.5 times and 2 times longer, respectively, in cocaine treated mice than controls. These results show for the first time the effects of cocaine on remodeling of dopamine circuitry and reveal new details on how dopamine neurons physical associate with downstream targets.

Introduction

It is well established that alterations in the mesocorticolimbic dopamine pathway, a neuromodulator circuit originating in the ventral tegmental area (VTA) and terminating in the nucleus accumbens (NAc), is central to the development of addictive behaviors (Berke and Hyman, 2000). In particular, cocaine, a powerful and addictive stimulant, is believed to elicit it’s addictive affect by physically binding to the dopamine transporter (DAT) on DA neurons preventing the reuptake of extracellular dopamine, resulting in

prolonged dopamine-mediated stimulation of target neurons (Ritz et al., 1987) and functional and structural plasticity in neurons of the mesocorticolimbic pathway. Cocaine-mediated changes in Long-term potentiation (LTP) and Long-term depression (LTD) have been reported in pathways upstream of DA neurons between excitatory inputs and dopamine dendrites in the VTA (Saal et al., 2003; Ungless et al., 2001) and downstream of DA neurons at synaptic sites of NAc-residing Medium spiny neurons (MSNs) (Huang et al., 2009; Thomas et al., 2001). Structurally, cocaine has been reported to increase the spine density in DA dendrites in the VTA (Sarti et al., 2007), and decreased dendritic branching and spine density of NAc MSNs (Alcantara et al., 2011; Barrientos et al., 2018).

However, there exists little information on how cocaine affects DA axons and connections. Part of the reason for this gap is the difficulty in characterizing connectivity in general and the connectivity of dopamine axons specifically since there is not a 'pathognomonic' anatomical signature of DA axons or their "connections" with targets (Liu et al., 2018; Rice and Cragg, 2008). Previous EM studies of DA axons, primarily limited to immuno-labeling approaches (Bérubé-Carrière et al., 2012; Moss and Bolam, 2008) of single 2D EM sections, report that TH+ (*i.e*. DA axons) are in close proximity to NAc dendrites, often receiving a second spine synapse from a VGLUT+ axon terminal. These putative points of contact between DA axons and NAc neurites showed weak expression of synaptic proteins (e.g. Gephyrin, PSD-95, AMPAR) and thus may represent points of molecularly organized physical interactions (Uchigashima et al., 2016). Finally, fluorescence labeling of DA axons suggested that DA axon form varicosities in close proximity to dendritic spines and the number of these dendritic-neighboring varicosities increased after acute cocaine treatment (Dos Santos et al., 2018). While suggestive, the lack of anatomical gold-standard markers classically used to define synaptic contacts (Harris and Weinberg, 2012) makes it difficult to tell whether the proximity of a DA axon to a neurite is conclusive the dendrite is a dopamine target. Thus, results on how cocaine modifies DA axon structure and potential synapses remains elusive.

We address this gap by combining recent advances in genetic labeling techniques for EM along with large volume, serial EM (i.e. "connectomics") (Kasthuri et al., 2015) to study how cocaine alters the structure of dopamine axons. Using the genetically encoded peroxidase gene, APEX2 (Joesch et al., 2016; Martell et al., 2017), we labeled VTA dopamine neurons in 2 cocaine sensitized and 3 control mice in serial EM datasets and reconstructed dopamine neurons in the VTA and their axons in the NAc (~0.5 mm x 0.5mm x 0.2mm volumes). We show that cocaine exposure causes widespread remodeling of DA axons with extensive branching and the formation of 'bulbs', reminiscent of retraction bulbs along with widespread changes in mitochondria in DA axons and their putative targets. Our findings give new insight into DA axon biology and help fill in a major gap in describing how cocaine impacts the meso-corticolimbic circuitry.

Results

We bilaterally injected Adeno-associated virus (AAV) encoding a CRE-dependent cytosolic or mitochondrial targeted APEX2 (Apex2) into the Ventral Tegmental Area (VTA) of 4 mice expressing CRE from the promoter of the dopamine transporter gene (DAT-CRE) (Backman et al., 2006). This strategy works, resulting in Apex2 expression in VTA-residing DA neurons that project axons to the Nucleus Accumbens (NAc) (Fig. 1A). Four weeks following AAV expression, mice were perfused and brain slices were treated 3,3′-Diaminobenzidine(DAB) to precipitate Apex2 and bind osmium tetroxide (Joesch et al., 2016; Martell et al., 2017). Brain sections with Apex2-precipitate in appropriate brain regions (NAc and VTA) were cut into smaller pieces (NAc, Fig. 1A, right green circles and VTA not shown) and further processed for serial EM (Hua et al., 2015)(see Methods). Single 2D EM sections confirmed that DA neurons were unambiguously and completely filled with Apex including the smallest processes, dendritic spine heads (Fig. 1B, middle panel, cyan arrow) and thin axonal processes several millimeters away from the injection site (Fig 1B, right panel). We found no evidence of labeled soma in any other brain region, including the NAc, suggesting that the viral strategy targeted genetically specified DA axons in an anterograde manner. In 2 animals, AAV Apex2 injections in DAT-CRE mice were followed four weeks later by an established cocaine sensitization protocol designed to uncouple the effects of cocaine from other conditioning behaviors associated with self-administration paradigms (Beeler et al., 2009). Briefly, mice were given one daily intraperitoneal (IP) injection of either cocaine (10 mg/kg) or equivalent volume of saline every other day for a total of 4 injections (Fig. 1C, left panel). Immediately following each cocaine injection, mice were place in a novel environment where locomotor activity was monitored. Figure 1d shows an example of the difference in animal movement between cocaine and saline treated groups after the first day of treatment (see Fig. S1 for full behavioral data). After the final injection, mice went through a four-day abstinence period before being sacrificed and brains processed for Apex2 staining and serial EM.

We first described ultra-structural features of the putative DA contacts with target neurons, i.e. what, if any, types of synapses did they make? We focused on 30 APEX2 labeled boutons from DA axons in the control and 20 from the cocaine treated mice throughout the EM volume and for each bouton, examined every neuron in membrane to membrane apposition for signs of synaptic specialization (i.e. synaptic vesicles, post-synaptic densities). In order to ensure that we did not miss relevant ultrastructural details, we also examined DA boutons in control animals where we injected an AAV containing a CRE-dependent mitochondrial targeted Apex2 into a DAT-CRE mouse. By targeting Apex2 to the mitochondria, we were able to unambiguously identify DA axons in the EM while also insuring complete visualizing of their internal contents (i.e. synaptic vesicles). Broadly, most DA boutons (% 65 or 67/102) contained a few synaptic vesicles but only in few ~2% (2/102) could we see any sign of post-synaptic density staining in any neurite in contact with the bouton, although PSDs were easy to identify in neighboring unlabeled excitatory axonal synapses. An interesting feature of DA axons in both Apex-cyto and Apex-Mito datasets was that 20% (21/102) boutons contained

invaginations, the majority of which either involved unlabeled axons (control: 83%, n=49/59 contact points scored across 19 axons; cocaine: 77%, n =56/73 contact points scored across 20 axons) or unlabeled dendrites (control: 17%, n=10/59 contact points scored across 19 axons; cocaine: 23%, n = 17/73 contact points scored across 19 axons) (Figure 2A-B). Of the unlabeled axons, 43% (6/13) made additional synapses on dendritic spines in the volume, suggesting they were excitatory and 57% made synapses on dendritic shafts with little sign of PSD, suggesting they were inhibitory. All dendrites contacted were 100% spiny. These invaginations were the main signs of physical interactions between DA axons and putative targets and we saw no evidence of innervation of dendritic spines, i.e. a DA bouton proximate to a spine (or shaft) with a clear post-synaptic density.

We then analyzed the trajectories of axons in 20 nm (x,y) resolution EM volumes from NAc datasets of 2 control (+saline) and 2 cocaine treated (+ cocaine) mice. We annotated 60 Apex2+ DA axons for a total length of 3,971.70 microns of DA axon analyzed. Immediately obvious from the axonal reconstructions was that DA axons after exposure to cocaine branched far more than controls (+ cocaine, red colored axons, +saline, blue hued axons; Figure 3A). Across labeled DA axons, there was an average 3.7-fold increase in branch number for similar axon lengths after exposure to cocaine than relative to control (Fig. 3B; mean branch number/axon: +saline, 0.72 mean, 0.33 SEM, n = 29 axons; +cocaine, 2.67 mean, 0.44 SEM, n = 30 axons. P = 1.87e-6, Mann-Whitney U test). We then investigated whether branching was accompanied by an increased number of putative post-synaptic contacts as described above. We found that while axonal branching was accompanied by an increase total number of contacts (i.e. interdigitations) with dendrites and axons, the number of contacts per length was same between cocaine exposed and control DA axons. (Figure 3C; mean number of contacts points/axon: +saline, 12.5 mean, 3.3 SEM, r^2 = 0.94, n = 125 contact points across 10 axons; +cocaine, 15.8 mean, 2.6 SEM, r^2 = 0.54, n = 142 contact points across 9 axons. P = 0.90, Mann-Whitney U test). Indeed, control axons showed a fairly regular and uniform distributions of contacts along the axon (Fig 3A), whereas in cocaine exposed and highly branched DA axons, there were large regions of axon that were devoid of any contacts (Figure 3A). Finally, we did not see an obvious difference in the distribution of interdigitations that were axo-axonic versus axo-dendritic or contained vesicles (control: 83% (49/59) axo-axonic, 17% (10/59) axo-dendritic; cocaine: 77% (56/73) axo-axonic, 23% (17/73) axo-dendritic), suggesting that while there were large changes in axonal structure and the numbers of synapses, there were minimal changes in how DA axons interacted with post-synaptic targets.

The second obvious feature of DA axons exposed to cocaine was the occurrence of large swellings or bulbs in the axon (Figure 4). The swellings were often >600 nanometers in diameter significantly larger than those associated with interdigitations (102 nanometers) described above. These ‘bulbs’ were common in the cocaine exposed animals ~56% (17/30 axons) but we did not see a single example in DA axons from control animals, suggesting that APEX2 expression alone does not cause these swellings (Figure 4A; mean swellings/axon: + saline, 0.00 mean, 0.00 SEM, n = 29 axons; +cocaine, 1.00 mean, 0.21 SEM, n = 30 axons. P = 8.0e-6, Mann-Whitney U

test). Figure 4B shows reconstructions of two of these axons with swellings (large spheres with asterisk). DA axons were found to have either a large swelling along the axon (bottom reconstruction), often surrounded by medium sized swellings (green spheres), or containing terminal bulbs (top reconstruction, asterisk) reminiscent of axon retraction bulbs observed in developing neuromuscular junctions and developing brains (Balice-Gordon et al., 1993; Bishop et al., 2004; Bixby, 1981; Korneliussen and Jansen, 1976; Riley, 1981). Interestingly, we did not observe such any swellings in any NAc dendrite or afferent axons (*i.e.* excitatory axons that make chemical synapses) coming from cortical and subcortical areas (Pennartz et al., 1994). Additionally, we did not observe any swellings in VTA DA dendrites despite also being sites of dopamine release (data not shown). We then re-imaged EM volumes around different swellings at a higher resolution (~6nm x,y). Figure 4C shows two examples (highlighted in red), one containing Apex (Apex+) and one that did not (Apex-). The Apex- axon was verified to structurally resemble DA axons (*i.e.* contained varicosities, did not make chemical synapses, nor dendritic spines). Both swellings were completely filled with elongated mitochondria (highlighted in blue) and surrounded by otherwise normal neuropil (example of dendrites and myelinated axons highlighted in green). When these bulbs were reconstructed into 3D renderings, we found the mitochondria to be extremely elongated and twisted when packed into the swelling (Figure 4D) and that nearly all bulbs examined were packed this way.

The tortuous and elongated nature of the mitochondria in these bulbs made us curious about possible mitochondrial changes in other cell types in the same tissue. One advantage of large volume EM datasets is that, since all cells and intracellular organelles like mitochondria are also labeled, we could ask whether cocaine altered mitochondrial length in other parts of DA neurons as well as other neurons in the NAc. We quantified mitochondrial lengths at five locations: (Figure 5A): in the NAc, we measured mitochondria length in: (a) Apex2+ DA axons, (b) axons that make chemical synapses (i.e. GLUT2 afferents) (CS axons), and (c) MSN dendrites and in the VTA, (d) Apex2+ DA soma and (e) Apex2+ DA dendrites. Consistent with the increased mitochondria lengths found in large DA axon swellings, Apex+ DA axons in the NAc had longer mitochondria throughout in the cocaine treated mouse compared to the saline control (Fig 5B top; mean mitochondria length: +saline, 0.37 mean, 0.1 μm SEM, n = 97 mitochondria across 17 axons; +cocaine, 1.32 mean, 0.32 μm SEM, n = 111 mitochondria across 20 axons. P = 5.62e-16, Mann-Whitney U test). Cocaine also resulted in increased mitochondrial length in NAc MSN dendrites, the putative targets of DA axons (Fig 5B middle; mean mitochondria length/dendrite diameter: +saline, 1.36 mean, 0.14 SEM, n = 102 mitochondria across 30 dendrites; +cocaine, 3.04 mean, 0.2 SEM, n = 220 mitochondria across 21 dendrites. P = 4.96e-6, Mann-Whitney U test). However, increased mitochondria length appeared to be specific to DA axons and MSN dendrites, as we observed no difference in mitochondrial length in Apex- NAc CS axons between cocaine and saline treated mice (Fig 5B bottom; mean mitochondria length: +saline, 0.54 mean, 0.04 μm SEM, n = 80 mitochondria across 18 axons; +cocaine, 0.92 mean, 0.07 μm SEM, n = 85 mitochondria across 17 axons. P = 0.09, Mann-Whitney U test). Surprisingly, we didn't not observe any differences in mitochondrial length in VTA Apex+ DA soma or dendrites as compared to controls (Fig. 5C top; mean

mitochondrial length in APEX+ DA Soma: +saline, 2.46 mean, 0.24 µm SEM, n = 70 mitochondria across 4 soma; +cocaine, 2.78 mean, 0.23 µm SEM, n = 141 mitochondria across 5 soma. P = 0.68, Mann-Whitney U test; Fig. 5Cc bottom; mean mitochondrial length/dendrite diameter (nm) in APEX+ DA dendrites: +saline, 1.74 mean, 0.25 SEM, n = 37 mitochondria across 4 dendrites; +cocaine, 1.85 mean, 0.22 SEM, n = 53 mitochondria across 10 dendrites. P = 0.57, Mann-Whitney U test). Lastly, we confirmed that cocaine did not increase the number of mitochondria in DA axons (Figure S2; mean number of mitochondria: +saline, 5.33 mean, 1.33 SEM mitochondria/axon, n = 96 mitochondria across 18 axons; + cocaine, 5.35 mean, 0.82 SEM mitochondria/axon, n = 107 mitochondria across 20 axons. P = 0.72, Mann-Whitney U test). Taken together, these results indicate that cocaine sensitization increases mitochondrial length in the mesolimbic pathway in both cell type specific manner (i.e. in DA axons and not in CS axons) but also in sub-cellular specific manner (DA axons and not DA soma and DA dendrites).

Discussion

We use genetic labeling of DA axons and large volume serial electron microscopy and present several novel results of dopamine circuitry and the effects of drugs of abuse like cocaine on that circuitry. First, we demonstrate how DA axons physically interact with other neurons. How neuromodulatory neurons interact with downstream targets has long been unclear likely due to EM immuno-labeling techniques often being limited to individual 2D EM sections. Using APEX2 labeling and automated serial EM, we demonstrate that the majority of DA axons lack obvious signs of synapses at most boutons and instead physically interdigitated with axons and dendrites. Given that DA axons lack vesicles at many of these contact sites, it's unclear how they correlate with dopamine release but as previous reports suggest that only 30% of DA axon varicosities contain the molecular machinery for active dopamine release (Liu et al., 2018), DA axons may shuttle dopamine vesicles to different varicosity sites. and future studies that correlate contact sites with DA activity of individual boutons would clarify this result. It is possible that other neuromodulatory circuits (i.e. serotonin, cholinergic, norepinephrine) use similar structures as a general anatomical feature of these cell types.

Second, we expand our current understanding of the structural changes following cocaine exposure in the brain. While previous reports have focused on changes in DA spine density in the VTA and MSN spine/synapse density in the NAc, our results fill in an important gap to our understanding of how cocaine alters the structure of the mesocorticolimbic circuit on the axonal side. Our data is consistent with active remodeling of dopamine axons: retraction bulbs on axon terminals in the process of pruning (i.e. removing connections) and increased branching (i.e. formation of new connections). These changes occurred after just days of exposure and days of withdrawal, suggesting rapid pace of these large scale anatomical changes. Follow-up studies that examine whether these alterations persist at longer time points or even in models of addiction would shed further light on how these re-arrangements correlated with long term behavioral changes. Finally, our data is consistent with the idea that the major structural change following exposure to cocaine is an increase in the number of

interactions between DA axons and targets as opposed to changes in the size or composition of individual connections.

Changes in DA axons in response to cocaine bare striking similarities with remodeling events observed during development and traumatic brain injury (TBI). Axonal bulbs in development and TBI (Johnson et al., 2013) have been distinguished from each other as either axon retraction or axon degeneration (Rosenthal and Taraskevich, 1977)(*i.e.* “Wallerian degeneration”), respectively (Bishop et al., 2004). Because we do not observe axon fragmentation, a hallmark of axon degeneration, but rather large bulbs connected to otherwise intact axons, the effects of cocaine on dopamine axons resemble more closely those seen during development with some notable differences. Axon retraction bulbs during development are often surrounded by glia to presumably remove contents of the pruned axon terminal (Bishop et al., 2004). However, we do not observe any glia on or near dopamine axon bulbs during this remodeling process. This could be differences in the biology of cocaine-induce and developmental axon bulbs, or the timing in which we sacrificed the mouse after cocaine sensitization. Another important distinction is that some of the large swellings in dopamine axons were not terminal bulbs like those seen in neuromuscular junctions. Because dopamine neurons are neuromodulatory neurons characterized by having varicosities along their axon lengths (Liu et al., 2018), we suspect bulbs in dopamine axons will form in both varicosities and terminal points.

Finally our results on changes in mitochondrial length provide a potential cellular substrate for studies implicating cocaine in altering aspects of brain energy homeostasis including changes in oxidative stress, cellular respiration, and enrichment of mitochondrial-related transcripts in NAc brain slice preps (Dietrich et al., 2005; Feng et al., 2014; Kalivas, 2009; Lehrmann et al., 2003; Volkow et al., 1991). Another possibility is that mitochondrial elongation is the result of the hyper activity of the mesolimbic circuit as demonstrated by the increased movement of mice exposed to cocaine. Future experiments where activity of neurons is tightly controlled, perhaps with optical stimulation, and then mitochondrial length is analyzed in those neurons could shed light on this possibility. The cell type specific nature of our results, i.e. DA axons show elongated mitochondria but excitatory, putative glutamate, axons do not suggest that mitochondrial change is perhaps related to DA specific activity. The increase in mitochondrial length in NAc dendrites is then because they are the targets of that axonal activity. Finally, our observation that mitochondrial changes are primarily seen in DA axons and not DA soma or dendrites could suggest either that cocaine acts directly on DA axons or that the major influence of cocaine is on axonal activity.

References

Alcantara, A.A., Lim, H.Y., Floyd, C.E., Garces, J., Mendenhall, J.M., Lyons, C.L., and Berlanga, M.L. (2011). Cocaine- and morphine-induced synaptic plasticity in the nucleus accumbens. Synapse 65, 309-320.

Backman, C.M., Malik, N., Zhang, Y., Shan, L., Grinberg, A., Hoffer, B.J., Westphal, H., and Tomac, A.C. (2006). Characterization of a mouse strain expressing Cre recombinase from the 3' untranslated region of the dopamine transporter locus. Genesis 44, 383-390.

Balice-Gordon, R.J., Chua, C.K., Nelson, C.C., and Lichtman, J.W. (1993). Gradual loss of synaptic cartels precedes axon withdrawal at developing neuromuscular junctions. Neuron 11, 801-815.

Barrientos, C., Knowland, D., Wu, M.M.J., Lilascharoen, V., Huang, K.W., Malenka, R.C., and Lim, B.K. (2018). Cocaine-Induced Structural Plasticity in Input Regions to Distinct Cell Types in Nucleus Accumbens. Biol Psychiatry 84, 893-904.

Beeler, J.A., Cao, Z.F., Kheirbek, M.A., and Zhuang, X. (2009). Loss of cocaine locomotor response in Pitx3-deficient mice lacking a nigrostriatal pathway. Neuropsychopharmacology 34, 1149-1161.

Berger, D.R., Seung, H.S., and Lichtman, J.W. (2018). VAST (Volume Annotation and Segmentation Tool): Efficient Manual and Semi-Automatic Labeling of Large 3D Image Stacks. Front Neural Circuits 12, 88.

Berke, J.D., and Hyman, S.E. (2000). Addiction, dopamine, and the molecular mechanisms of memory. Neuron 25, 515-532.

Bishop, D.L., Misgeld, T., Walsh, M.K., Gan, W.B., and Lichtman, J.W. (2004). Axon branch removal at developing synapses by axosome shedding. Neuron 44, 651-661.

Bixby, J.L. (1981). Ultrastructural observations on synapse elimination in neonatal rabbit skeletal muscle. J Neurocytol 10, 81-100.

Bérubé-Carrière, N., Guay, G., Fortin, G.M., Kullander, K., Olson, L., Wallén-Mackenzie, Å., Trudeau, L.E., and Descarries, L. (2012). Ultrastructural characterization of the mesostriatal dopamine innervation in mice, including two mouse lines of conditional VGLUT2 knockout in dopamine neurons. Eur J Neurosci 35, 527-538.

Dietrich, J.B., Mangeol, A., Revel, M.O., Burgun, C., Aunis, D., and Zwiller, J. (2005). Acute or repeated cocaine administration generates reactive oxygen species and induces antioxidant enzyme activity in dopaminergic rat brain structures. Neuropharmacology 48, 965-974.

Dos Santos, M., Cahill, E.N., Bo, G.D., Vanhoutte, P., Caboche, J., Giros, B., and Heck, N. (2018). Cocaine increases dopaminergic connectivity in the nucleus accumbens. Brain Struct Funct 223, 913-923.

Feng, J., Wilkinson, M., Liu, X., Purushothaman, I., Ferguson, D., Vialou, V., Maze, I., Shao, N., Kennedy, P., Koo, J.*, et al.* (2014). Chronic cocaine-regulated epigenomic changes in mouse nucleus accumbens. Genome Biol 15, R65.

Harris, K.M., and Weinberg, R.J. (2012). Ultrastructure of synapses in the mammalian brain. Cold Spring Harb Perspect Biol 4.

Hua, Y., Laserstein, P., and Helmstaedter, M. (2015). Large-volume en-bloc staining for electron microscopy-based connectomics. Nat Commun 6, 7923.

Huang, Y.H., Lin, Y., Mu, P., Lee, B.R., Brown, T.E., Wayman, G., Marie, H., Liu, W., Yan, Z., Sorg, B.A.*, et al.* (2009). In vivo cocaine experience generates silent synapses. Neuron 63, 40-47.

Joesch, M., Mankus, D., Yamagata, M., Shahbazi, A., Schalek, R., Suissa-Peleg, A., Meister, M., Lichtman, J.W., Scheirer, W.J., and Sanes, J.R. (2016). Reconstruction of genetically identified neurons imaged by serial-section electron microscopy. Elife 5.
Johnson, V.E., Stewart, W., and Smith, D.H. (2013). Axonal pathology in traumatic brain injury. Exp Neurol 246, 35-43.
Kalivas, P.W. (2009). The glutamate homeostasis hypothesis of addiction. Nat Rev Neurosci 10, 561-572.
Kasthuri, N., Hayworth, K.J., Berger, D.R., Schalek, R.L., Conchello, J.A., Knowles-Barley, S., Lee, D., Vazquez-Reina, A., Kaynig, V., Jones, T.R.*, et al.* (2015). Saturated Reconstruction of a Volume of Neocortex. Cell 162, 648-661.
Korneliussen, H., and Jansen, J.K. (1976). Morphological aspects of the elimination of polyneuronal innervation of skeletal muscle fibres in newborn rats. J Neurocytol 5, 591-604.
Lehrmann, E., Oyler, J., Vawter, M.P., Hyde, T.M., Kolachana, B., Kleinman, J.E., Huestis, M.A., Becker, K.G., and Freed, W.J. (2003). Transcriptional profiling in the human prefrontal cortex: evidence for two activational states associated with cocaine abuse. Pharmacogenomics J 3, 27-40.
Liu, C., Kershberg, L., Wang, J., Schneeberger, S., and Kaeser, P.S. (2018). Dopamine Secretion Is Mediated by Sparse Active Zone-like Release Sites. Cell 172, 706-718.e715.
Martell, J.D., Deerinck, T.J., Lam, S.S., Ellisman, M.H., and Ting, A.Y. (2017). Electron microscopy using the genetically encoded APEX2 tag in cultured mammalian cells. Nat Protoc 12, 1792-1816.
Marx, A., Backes, C., Meese, E., Lenhof, H.P., and Keller, A. (2016). EDISON-WMW: Exact Dynamic Programing Solution of the Wilcoxon-Mann-Whitney Test. Genomics Proteomics Bioinformatics 14, 55-61.
Moss, J., and Bolam, J.P. (2008). A dopaminergic axon lattice in the striatum and its relationship with cortical and thalamic terminals. J Neurosci 28, 11221-11230.
Pennartz, C.M., Groenewegen, H.J., and Lopes da Silva, F.H. (1994). The nucleus accumbens as a complex of functionally distinct neuronal ensembles: an integration of behavioural, electrophysiological and anatomical data. Prog Neurobiol 42, 719-761.
Rice, M.E., and Cragg, S.J. (2008). Dopamine spillover after quantal release: rethinking dopamine transmission in the nigrostriatal pathway. Brain Res Rev 58, 303-313.
Riley, D.A. (1981). Ultrastructural evidence for axon retraction during the spontaneous elimination of polyneuronal innervation of the rat soleus muscle. J Neurocytol 10, 425-440.
Ritz, M.C., Lamb, R.J., Goldberg, S.R., and Kuhar, M.J. (1987). Cocaine receptors on dopamine transporters are related to self-administration of cocaine. Science 237, 1219-1223.
Rosenthal, J.L., and Taraskevich, P.S. (1977). Reduction of multiaxonal innervation at the neuromuscular junction of the rat during development. J Physiol 270, 299-310.
Saal, D., Dong, Y., Bonci, A., and Malenka, R.C. (2003). Drugs of abuse and stress trigger a common synaptic adaptation in dopamine neurons. Neuron 37, 577-582.
Sarti, F., Borgland, S.L., Kharazia, V.N., and Bonci, A. (2007). Acute cocaine exposure alters spine density and long-term potentiation in the ventral tegmental area. Eur J Neurosci 26, 749-756.
Thomas, M.J., Beurrier, C., Bonci, A., and Malenka, R.C. (2001). Long-term depression in the nucleus accumbens: a neural correlate of behavioral sensitization to cocaine. Nat Neurosci 4, 1217-1223.

Uchigashima, M., Ohtsuka, T., Kobayashi, K., and Watanabe, M. (2016). Dopamine synapse is a neuroligin-2-mediated contact between dopaminergic presynaptic and GABAergic postsynaptic structures. Proc Natl Acad Sci U S A 113, 4206-4211.
Ungless, M.A., Whistler, J.L., Malenka, R.C., and Bonci, A. (2001). Single cocaine exposure in vivo induces long-term potentiation in dopamine neurons. Nature 411, 583-587.
Volkow, N.D., Fowler, J.S., Wolf, A.P., Hitzemann, R., Dewey, S., Bendriem, B., Alpert, R., and Hoff, A. (1991). Changes in brain glucose metabolism in cocaine dependence and withdrawal. Am J Psychiatry 148, 621-626.

Materials and Methods

Animals and AAV viruses

DAT-CRE mice ~15 weeks used in this study were acquired from Xiaoxi Zhuang, The University of Chicago, and can also be found at Jackson Laboratory (https://www.jax.org/strain/020080). AAV-CAG-DIO-APEX2NES (Cyto-Apex) was acquired as a gift from the laboratory of Joshua Sanes (Harvard) and is now available at Addgene: #79907. AAV-CAG-DIO-APEX2-MITO was generated in our lab by cloning the mitochondrial targeting sequencing from mito-V5-APEX2 (Addgene #72480) and placing it on the 5' end of APEX2-NES in AAV-CAG-DIO-APEX2NES. Finally, the nuclear export sequence (NES) was removed from APEX2. AAV virus was generated at the University of North Carolina School of Medicine Vector Core facility (https://www.med.unc.edu/genetherapy/vectorcore/). Animal care, perfusion procedures, and AAV injections were followed according to animal regulations at the University of Chicago's Animal Resources Center (ARC) and approved IACUC protocols.

AAV injections

AAV injections were performed using a standard stereotaxic frame. 70-100 nl of virus (~2.9×10^{12} viral genomes/ml) were bilaterally injected into the VTA using the stereotactic coordinates: 3.1 posterior of bregma, 0.55 lateral bregma, and 4.4 ventral of the dura. Mice were aged 4 weeks to allow for AAV expression before perfusion or cocaine sensitization experiments.

Cocaine sensitization

Mice were given a once daily intraperitoneal (IP) injection of either cocaine (10 mg/kg) or equivalent volume of saline every other day for a total of 4 injections. Immediately following each injection, mice were place in a novel environment where their locomotor activity was automatically monitored for one hour and then returned to their home cage.

Apex2 staining and EM preparation.

Brains were prepared in the same manner and as previously described (Hua et al., 2015). Briefly, an anesthetized animal was first transcardially perfused with 10ml 0.1 M

Sodium Cacodylate (cacodylate) buffer, pH 7.4 (Electron microscopy sciences (EMS) followed by 20 ml of fixative containing 2% paraformaldehyde (EMS), 2.5% glutaraldehyde (EMS) in 0.1 M Sodium Cacodylate (cacodylate) buffer, pH 7.4 (EMS). The brain was removed and placed in fixative for at least 24 hours at 4ºC. A series of 300 µm vibratome sections were prepared and put into fixative for 24 hours at 4ºC. Apex2 precipitation and polymerization was performed by washing slices extensively in cacodylate buffer at room temperature, incubated in 50mg/ml 3,3'diaminobenzidine (DAB) for 1 hour at room temperature followed with DAB/0.03% (v/v) H_20_2 until a visible precipitate forms (15-20 minutes). Slices were washed extensively in cacodylate buffer. Slices were reduced in 0.8 %(w/v) Sodium Hydrosulfite in 60%(v/v) 0.1 M Sodium Bicarbonate 40 %(v/v) 0.1 M Sodium Carbonate buffer for 20 minutes and washed in cacodylate buffer. Brain slices that showed prominent Apex2 staining in the correct anatomical location were cut into smaller pieces surrounding the Apex2 positive tissue (*i.e.* NAc and VTA) and prepared for EM by staining sequentially with 2% osmium tetroxide (EMS) in cacodylate buffer, 2.5% potassium ferrocyanide (Sigma-Aldrich), thiocarbohydrazide, unbuffered 2% osmium tetroxide, 1% uranyl acetate, and 0.66% Aspartic acid buffered Lead (II) Nitrate with extensive rinses between each step with the exception of potassium ferrocyanide. The sections were then dehydrated in ethanol and propylene oxide and infiltrated with 812 Epon resin (EMS, Mixture: 49% Embed 812, 28% DDSA, 21% NMA, and 2.0% DMP 30). The resin-infiltrated tissue was cured at 60ºC for 3 days. Using a commercial ultramicrotome (Powertome, RMC), the cured block was trimmed to a ~1.0mm x 1.5 mm rectangle and ~2,000, 40nm thick sections were collected from each block on polyamide tape (Kapton) using an automated tape collecting device (ATUM, RMC) and assembled on silicon wafers as previously described (Kasthuri et al., 2015). The serial sections were acquired using backscattered electron detection with a Gemini 300 scanning electron microscope (Carl Zeiss), equipped with ATLAS software for automated wafer imaging. Dwell times for all datasets were 1.0 microsecond. For 20nm and 6nm resolution data sets, sections were brightness/contrast normalized and rigidly aligned using TrakEM2 (FIJI) followed by non-linear affine alignment using AlignTK on Argonne National Laboratory's super computer, Cooley. Different image processing tools were packaged into Python scripts that can be found here: https://github.com/Hanyu-Li/klab_utils.

Data Analysis

Aligned datasets were manually skeletonized and annotated using the publicly available software, Knossos (https://knossos.app). Classes of cell types were identified by distinguishing anatomical properties: Apex2+ DA neurons (Soma and dendrites in the VTA and axons in NAc) were identified by their dark precipitate, Medium spiny neurons in the NAc by the presence of dendritic spines, and chemical synapse axons in the NAc by their formation of synapses on dendritic spines. Skeleton information was exported into tab delimited matrices using homemade Python scripts that compute skeleton features from the Knossos xml annotation file. Code is freely available here: https://github.com/knorwood0/MNRVA. Quantification and plotting of different anatomical features were performed in Matlab and excel. Two-tailed Mann Whitney U statistics test was used to test for significance (Marx et al., 2016).

Mitochondria length

The length of mitochondria was measured in Knossos by measuring along the longest axis from one of the three orthogonal views (xy,xz,yx). Dendrite diameter was measured by centering the mitochondria in the Knossos viewing window and then taking the average diameter between all three orthogonal axes.

Contact points

Contact points were found by tracing Apex2+ DA axons and marking in Knossos every point where an Apex2 negative neurite interdigitated with the DA axon. Interdigitation was determined by observing a neurite entering a DA axon and disappearing in the image stack using the three orthogonal views of Knossos. Neurites that passed over DA axons were not scored as contact points.

3D rendering

3D manual segmentation was done using VAST (Berger et al., 2018) and exported using MATLAB as .OBJ files which were then imported and rendered using Blender 2.79.

Figure 1

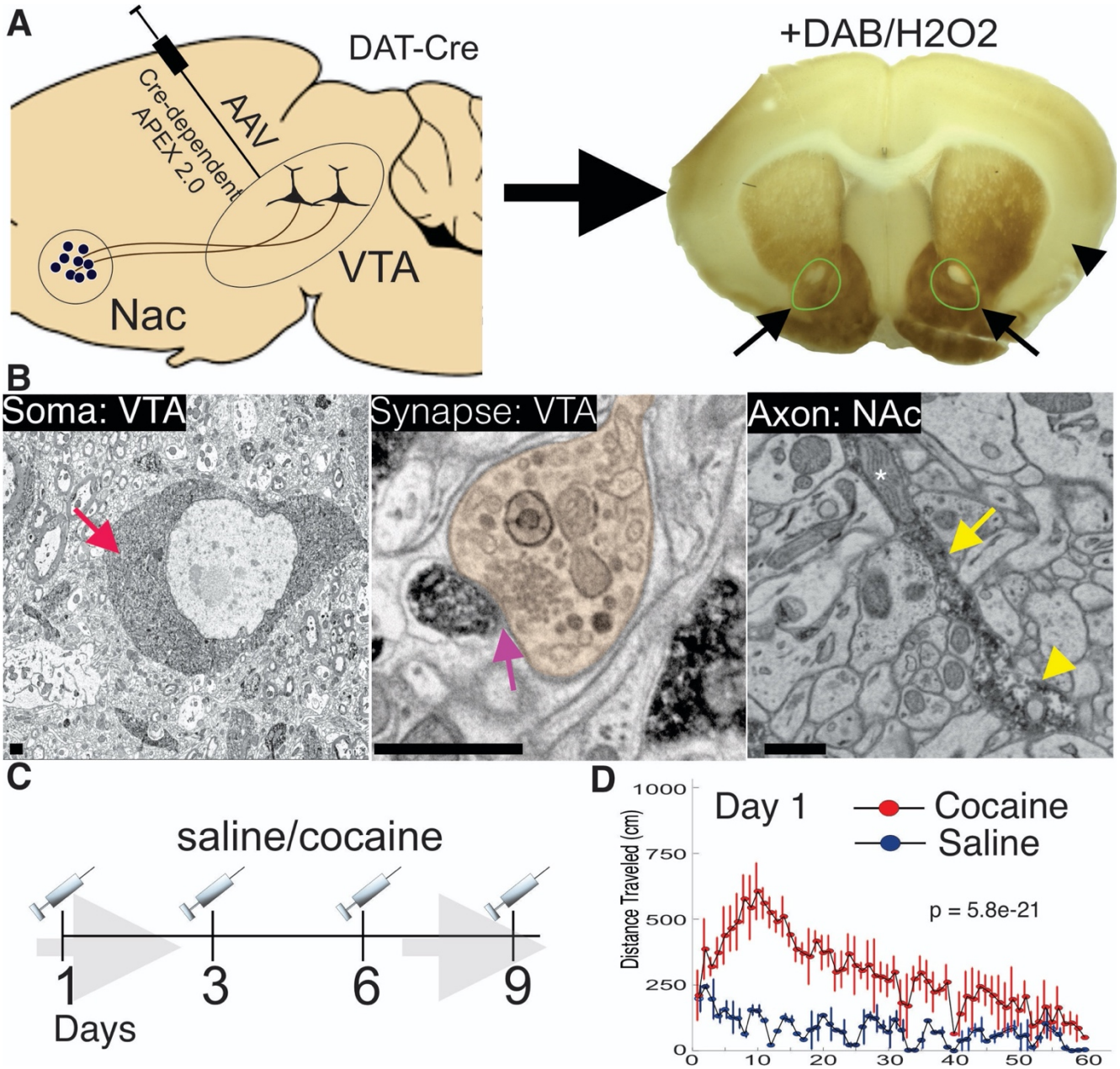
A
DAT-Cre
Cre-dependent
APEX 2.0
AAV
VTA
Nac
+DAB/H2O2
B
Soma: VTA
Synapse: VTA
Axon: NAc
C
saline/cocaine
1
3
6
9
Days
D
Day 1
Cocaine
Saline
p = 5.8e-21
Distance Traveled (cm)
1000
750
500
250
0
0
10
20
30
40
50
60

Figure 1. Experimental design for Dopamine connectomics. (**A**) AAVs expressing Cre-dependent Apex2 was biolaterally injected into the Ventral Tegmental Area (VTA) of transgenic mice expressing Cre in Dopamine Transporter positive neurons (DAT-CRE). ~4 weeks after AAV injections, vibratome sections (~300 microns thick) show strong Apex2 labeling in VTA after staining with 3'3'-Diaminobenzidene (DAB) and Hydrogen Peroxide (H202) before EM processing (see Methods). Black arrows point to an Apex2 positive region and black arrowhead points to an Apex2 negative region. Green circles highlight the NAc region dissected out and processed for EM. (**B**) Representative EM images of cytoplasmic Apex2: Left panel: Apex2 Soma in the VTA (red arrow); *Middle panel*: Apex2 dendritic spine forming a synapse (purple arrow) with presynaptic bouton (orange) in the VTA; *Right panel*: Apex2 axon in the NAc with narrow (yellow arrow) and thick varicosities (yellow arrowhead). Apex2 does not fill up mitochondria (asterix). (**C**) Cartoon depicting cocaine sensitization protocol: Mice received a single intraperitoneal (IP) injection of cocaine (10 mg/kg) or saline, placed in a novel cage environment, and their locomoter activity was monitored for 1 hr. This procedure was repeated every 3rd day for 4 rounds of injections. 4 days following the last injection (e.g. Day 13), mice were perfused and brains processed for Apex2/EM staining (see A and Methods). (**D**) Scatter plot of the average distance traveled (cm) versus time for the first day of cocaine or saline injection (n = 3 mice for each condition, error bars = standard deviation of the mean, P = 5.8e-21). Scale bar = 1 μm.Data: mean ± SEM. P-value: Mann-Whitney U test.

Figure 2

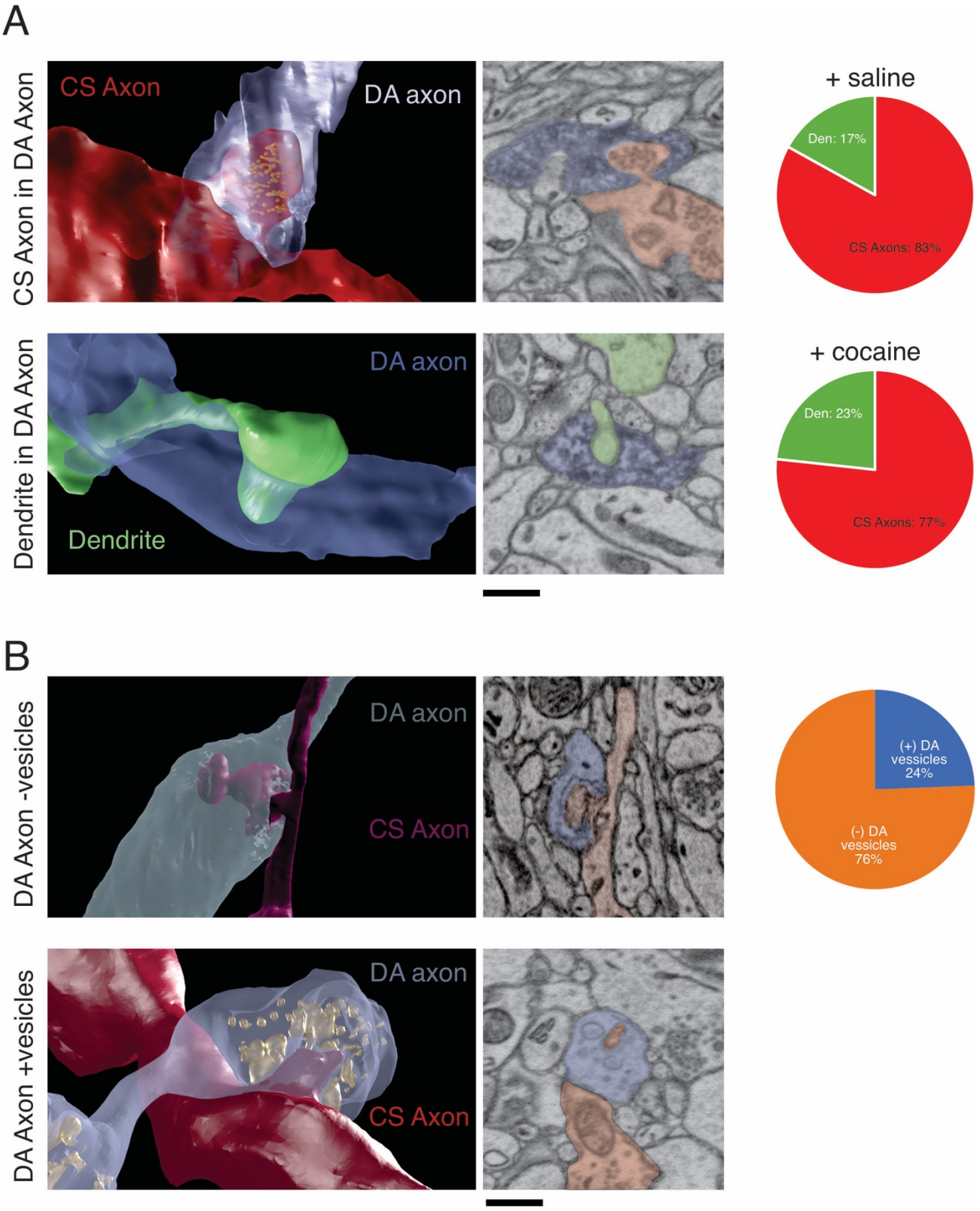
A
CS Axon in DA Axon
CS Axon
DA axon
+ saline
Den: 17%
CS Axons: 83%
Dendrite in DA Axon
DA axon
Dendrite
+ cocaine
Den: 23%
CS Axons: 77%
B
DA Axon -vesicles
DA axon
CS Axon
(+) DA vessicles 24%
(-) DA vessicles 76%
DA Axon +vesicles
DA axon
CS Axon

Figure 2. Dopamine contact points are physical interdigitations between DA axons and either NAc dendrites or conventional axons. (**A**) 3D renderings and matched 2D EM images of contact points between APEX+ DA axons (blue) and chemical synapse (CS) axons (red) (top panel) and APEX+ DA axons (blue) and dendrites (green) (bottom panel). *Right*: Pie charts showing proportion of contact points that are with CS axons and dendrites in saline and cocaine treated mice (+ saline: X APEX+ DA axons were reconstructed and X contact points scored; + cocaine: X APEX+ DA axons were reconstructed and X contact points scored). (**B**) 3D renderings and matched EM image from a wild mouse expressing Mito-APEX in DA neurons showing contact points between DA axons and conventional axons where DA axon varicosities are either empty (top panel) or contain vesicles (bottom panel). Pie chart showing proportion of DA axons with and without vesicles as the site of contact points between DA axons and conventional axons (X APEX+ DA axons were reconstructed and X contact points scored). Scale bar = 500 nm.

Figure 3

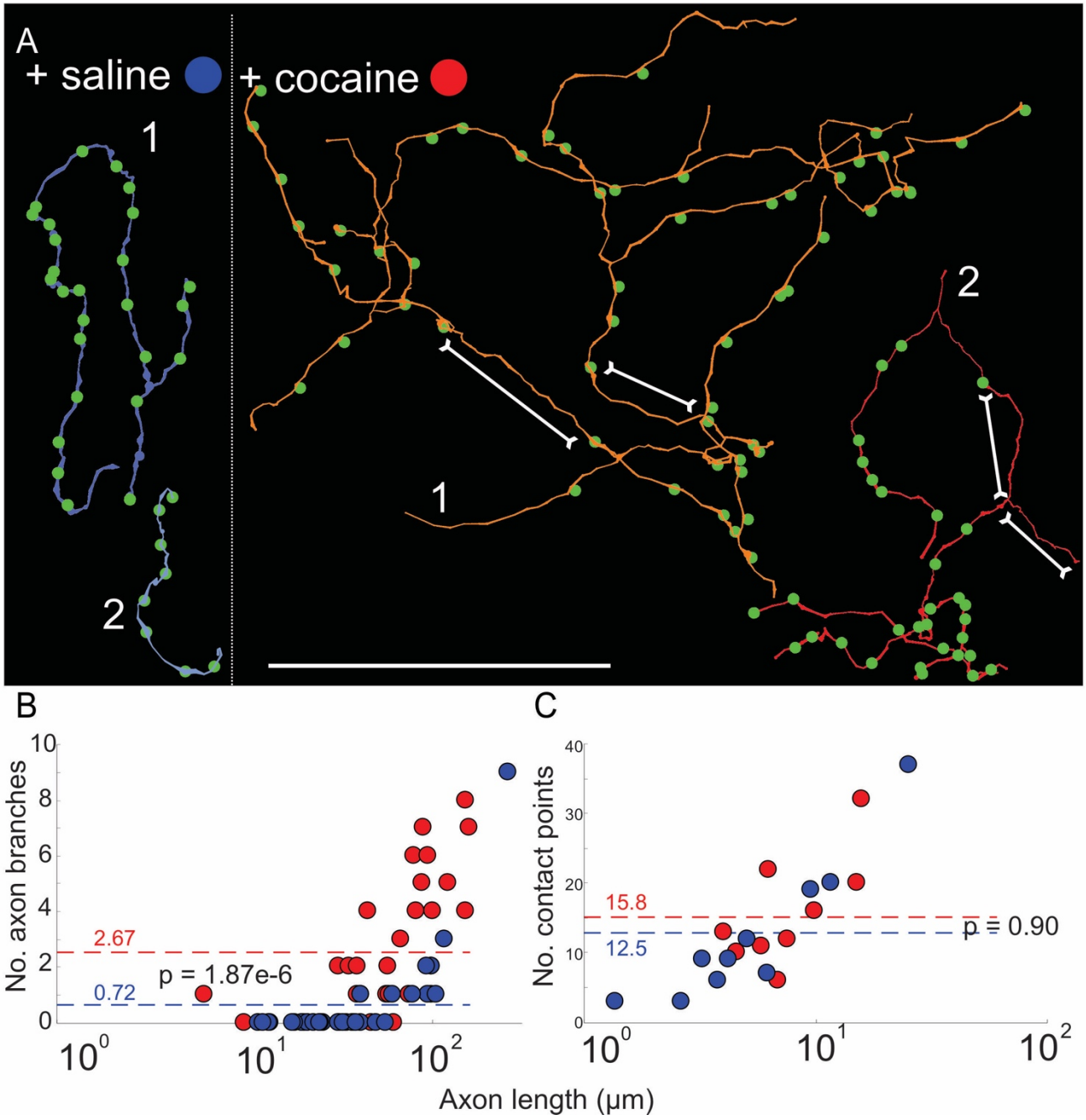
A
+ saline
+ cocaine
1
2
1
2
B
No. axon branches
2.67
0.72
p = 1.87e-6
C
No. contact points
15.8
12.5
p = 0.90
Axon length (μm)

Figure 3. Cocaine increases branching of Apex2 dopamine axons in cocaine sensitized mice. (A) Two representative reconstructions of DA axons each from saline (left, blue) and cocaine (right, red) treated mice. Green circles represent contact points where other neurons interdigitate with the DA axon. (**B**) Scatter plot of the number of DA axons branches versus axon length (μm) (+saline: 0.72 ± 0.33 branches/axon, n = 29 axons; +cocaine: 2.67 ± 0.44 branches/axon, n = 30 axons. P = 4.45e-5. (**C**) Scatter plot of the number of contact points versus total length of axon (+saline: 12.5 ± 3.3 contact points/axon, n = 125 contact points over 10 axons, r^2 = 0.94; +cocaine: 15.8 ± 2.6 contact points/axon, n = 142 contact points over 9 axons, r^2 = 0.54. P =0.9). Data: mean ± SEM. *P*-values: two-tailed Mann-Whitney U test.

Figure 4

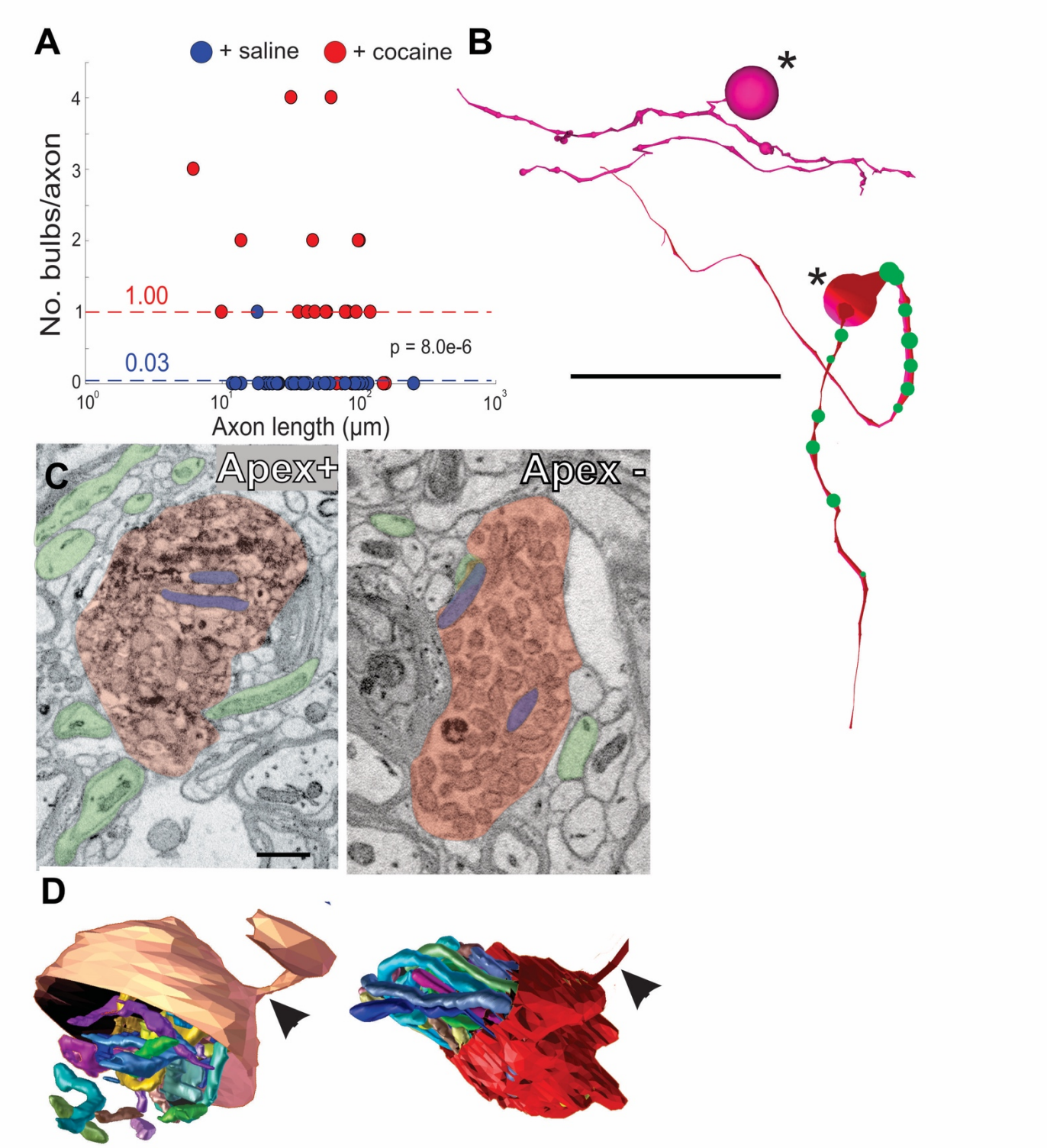
A
+ saline
+ cocaine
No. bulbs/axon
1.00
0.03
p = 8.0e-6
Axon length (μm)
B
C
Apex+
Apex -
D

Figure 4. Cocaine results in the formation of large swellings filled with mitochondria in Apex2+ DA axons. (**A**) Scatter plot of the number of large swellings versus axon length (μm) (+ saline: 0.03 ± 0.03 swellings/axon, n = 29 axons; + cocaine: 1.00 ± 0.21 swellings/axon, n = 30 axons. P = 6.82e-6. (**B**) Reconstructions of two representative Apex+ Dopamine axons with large swellings (asterix) and medium sized swellings (green spheres). Top reconstruction depicts an axon with a terminal axon bulb and bottom reconstruction shows one along the axon. (**C)** 2D EM images of Apex+ (top) and Apex- (bottom) large swellings (red) found in the NAC of cocaine treated animals. Both swellings are filled with mitochondria (examples highlighted in blue). Swellings are surrounded by local dendrites and axons (examples in green). (**D**) 3D segmentation of swellings from (B); Swellings are filled with extremely long and coiled mitochondria and each swelling is attached to a thin axon (arrowheads). Scale bar: (B) 20 μm, (C) 500 nm Data: mean ± SEM. *P*-values: two-tailed Mann-Whitney U test.

Figure 5

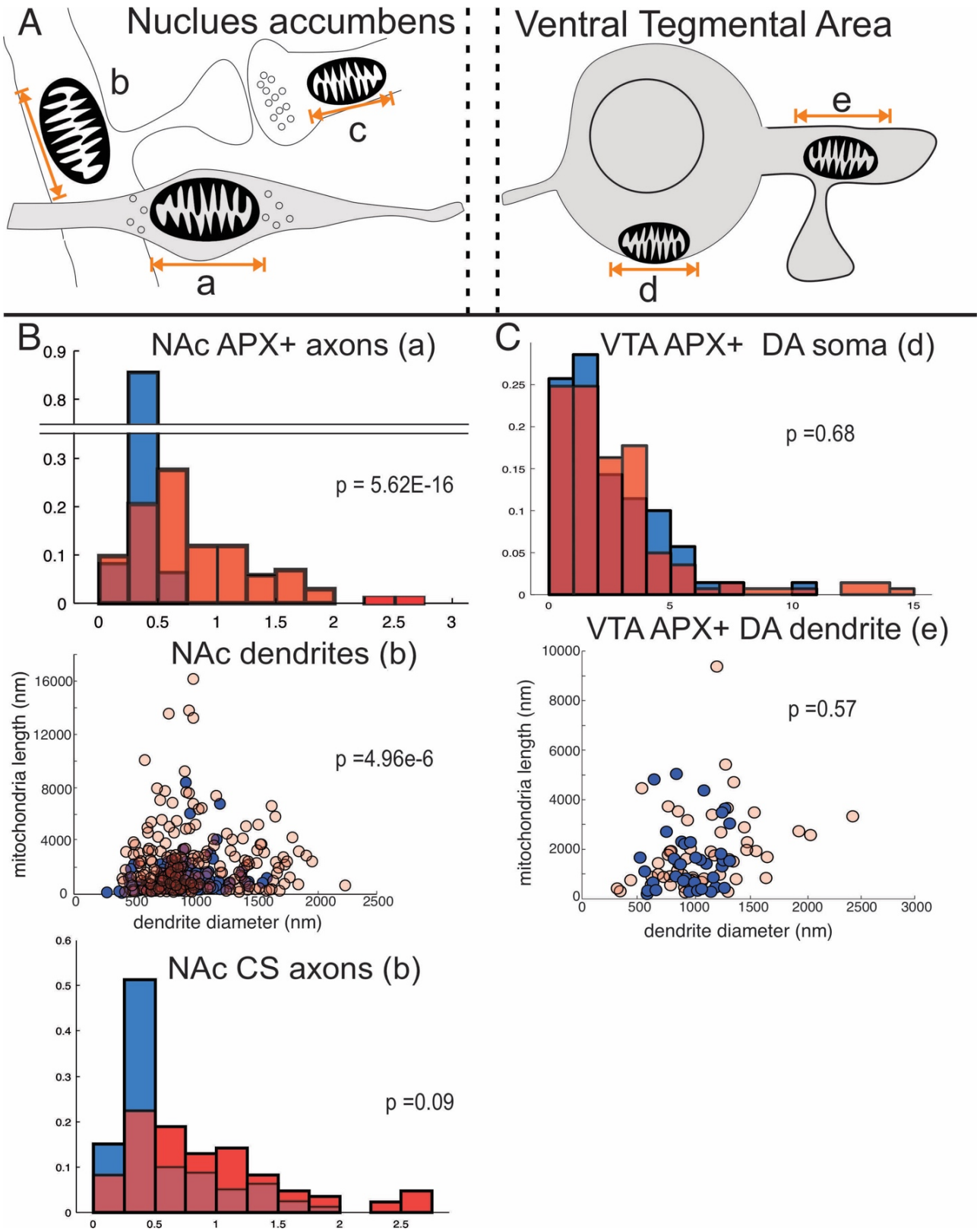
A
Nuclues accumbens
Ventral Tegmental Area
a
b
c
d
e
B
NAc APX+ axons (a)
p = 5.62E-16
NAc dendrites (b)
p =4.96e-6
mitochondria length (nm)
dendrite diameter (nm)
NAc CS axons (b)
p =0.09
C
VTA APX+ DA soma (d)
p =0.68
VTA APX+ DA dendrite (e)
p =0.57
mitochondria length (nm)
dendrite diameter (nm)

Figure 5. Cocaine results in increased mitochondria length in DA axons and MSN dendrites. (**A**) Cartoon depicting neurons we measured mitochondrial length: *Left*: in the NAc, we measured mitochondria in: (a) Apex2+ DA axons, (b) MSN dendrites, and (c) excitatory axons making chemical synapses (CS axons). *Right*: in the VTA, we measured mitochondria in: (d) Apex2+ DA soma, and (e) Apex2+ DA dendrites. (**B**) *Top*: histogram of mitochondria length in Apex2+ DA axons (+saline: 0.37 ± 0.1 μm, n = 97 mitochondria across 17 axons; + cocaine: 1.32 ± 0.32 μm, n = 111 mitochondria across 20 axons. P = 5.62 e-16. *Middle*: scatter plot of mitochondria lengths versus dendrite diameter of NAc MSN dendrites (+ saline: 1.36 ± 0.14 mito length/dendrite diameter (nm), n =102 mitochondria across 30 dendrites; + cocaine: 3.04 ± 0.2 μm, n = 220 mitochondria across 21 dendrites. P = 4.96e-6). *Bottom*: histogram of mitochondria lengths in NAc CS axons (+ saline: 0.54 ± 0.04 μm, n = 80 mitochondria across 18 axons; + cocaine: 0.92 ± 0.07 μm, n = 85 mitochondria across 17 axons. P = 0.09). (C) *Top*: Histogram of mitochondria length in Apex2+ DA Soma (+ saline: 2.46 ± 0.24 μm, n = 70 mitochondria across 4 soma; + cocaine: 2.78 ± 0.23 μm, n = 141 mitochondria across 5 soma. P = 0.68). *Bottom*: scatter plot of mitochondria lengths versus dendrite diameter of VTA Apex2+ DA dendrites (+saline: 1.74 ± 0.25 mito length/dendrite diameter (nm), n = 37 mitochondria across 4 dendrites; + cocaine: 1.85 ± 0.22 mito length/dendrite diameter (nm), n = 53 mitochondria across 10 dendrites. P = 0.57. Data: mean ± SEM. P-value: Mann-Whitney U test.